Tuning topological disorder in MgB$_2$

D. Di Castro,[1] E. Cappelluti,[2,3] M. Lavagnini,[3] A. Sacchetti,[1] A.Palenzona,[4] M. Putti,[4] and P. Postorino[1]

[1]*Coherentia-INFM-CNR and Physics Department,*
University of Rome "La Sapienza", P.le A. Moro 5, I-00185, Rome, Italy
[2]*SMC-Institute for Complex System, INFM-CNR, v. dei Taurini 19, 00185 Rome, Italy*
[3]*Physics Department, University of Rome "La Sapienza", P.le A. Moro 5, I-00185, Rome, Italy*
[4]*INFM-LAMIA, Dipartimento di Fisica, Via Dodecaneso 33, 16146 Genova, Italy*

We carried out Raman measurements on neutron-irradiated and Al-doped MgB$_2$ samples. The irradiation-induced topological disorder causes an unexpected appearance of high frequency spectral structures, similar to those observed in lightly Al-doped samples. Our results show that disorder-induced violations of the selection rules are responsible for the modification of the Raman spectrum in both irradiated and Al-doped samples. Theoretical calculations of the phonon density of states support this hypothesis, and demonstrate that the high frequency structures arise mostly from contributions at $\mathbf{q} \neq 0$ of the E$_{2g}$ phonon mode.

A few years after the discovery of superconductivity in MgB$_2$, many of its characteristic properties have been investigated and mostly clarified. Nowadays a wide consensus exists about MgB$_2$ being a phonon-mediated two-gap/two-band superconductor [1, 2, 3, 4, 5], where superconductivity mainly arises from the coupling of the holes in the σ band with the E$_{2g}$ phonon mode, which involves the in-plane stretching vibrations of boron atoms [6, 8, 9, 10]. In order to identify the fundamental mechanisms of the superconducting pairing, a key role has been played by a variety of experimental techniques which permitted the tuning of the electronic and lattice properties of MgB$_2$, such as the application of external pressure [11, 12], irradiation-induced disorder [13, 14, 15], chemical substitution (e.g. Al on the Mg-site [16, 17] and C on the B-site [18, 19]). In many of these cases, a reduction of the critical temperature, or even a suppression of the superconducting phase, have been observed. In doped MgB$_2$ compounds, in particular, the debate focuses on the relevance and the relative weight of two different microscopic mechanisms responsible for the reduction of T_c, namely the band filling effects which tune the electron density of states [20, 21, 22] and the disorder-induced increase of the inter-band scattering [7, 23].

Since the early investigations on MgB$_2$, Raman spectroscopy has been widely applied because the doubly degenerate E_{2g} mode, responsible for superconductivity, is the only Raman active among the four optical phonons (A$_{2u}$, B$_{1g}$, E$_{1u}$ and E$_{2g}$)[10, 24]. Indeed, the most prominent feature of the measured Raman spectrum, namely the very broad peak (width ~ 300 cm^{-1}) centered at around 620 cm^{-1} [11, 24, 25, 26]), has been generally identified with the E_{2g} phonon peak, whose predicted frequency at the zone center Γ lies within the 510-660 cm^{-1} range [6, 27]. Despite the almost general consensus on the above assignment, however, there remains unsolved controversies [24, 28, 29]. Most of the doubts arises from the anomalously large phonon linewidth and from its re-

markable temperature dependence [24, 25, 26, 30]. Different mechanisms, based on the strong electron-phonon (e-ph) coupling and on anharmonic effects, have been invoked to explain these features [11, 25, 26, 31, 32], although recent theoretical calculations suggest these effects do not fully account for the experimental findings [29]. As an alternative idea, the anomalously large line-shape was proposed to be related to the excitations of phonons outside the Γ point activated by lattice defects and multiphonon scattering [29]. This hypothesis has also been suggested by some experimental works where the large phonon line-shape [28], and other weak spectral features in the Raman spectrum [25], were ascribed to phonon contributions, throughout the Brillouin zone, activated by disorder-induced relaxation of the Raman selection rules.

Raman experiments have been also carried out on pure and doped MgB$_2$ films [32, 33, 34] and on bulk chemically substituted MgB$_2$ compounds [17, 18, 19, 25]. Also in these cases, the attempts at a quantitative analysis lead to ambiguous and sometime contradictory results. Contrary to the prediction of one Raman-active mode only, the introduction of even small quantities of substitutional impurities appears to drive the onset of additional high-frequency (HF) structures around 750 and 850 cm^{-1} [17, 19, 25], which are absent or vanishingly small in the pure compound. At higher levels of substitution, the Raman signal further complicates, progressively approaching the spectrum of the end compound. In Mg$_{1-x}$Al$_x$B$_2$ a two-steps behaviour is observed: the HF structures are well detectable at $x = 0.05$ and, up to $x = 0.25$, their intensity increases while keeping almost constant the frequency positions; for $x > 0.25$ the intensities keep growing but the frequencies increase and the lineshapes narrow, evolving as a whole towards the spectrum of the parent compound AlB$_2$ [17, 25]. However, since C and Al doping induces, at the same time, charge doping, volume compression and on-site lattice disorder,

it is particularly difficult to disentagle their effects on the Raman spectrum and on the superconducting properties.

The present paper aims to single out the effect of topological disorder by carring out a Raman study of differently neutron irradiated MgB_2 samples [15]. We show that neutron irradiation causes the appearance of HF spectral structures, similar to those observed in lightly Al-doped samples. The comparison of the present spectra with the literature data allows us to ascribe the unexpected HF Raman features, present in the irradiated and lightly Al-doped sample, to a disorder-induced violation of the Raman selection rules. Theoretical calculations of the phonon dispersion curves support this hypothesis and allow us to compare the Raman results with differently **q**-integrated phonon density of states (PDOS).

Isotopically enriched (^{11}B) polycrystalline MgB_2 was prepared by direct synthesis from pure elements Three identical samples were irradiated by means of thermal neutrons at the source SINQ (Paul Sherrer Institut, Switzerland) [15]. Different irradiation times were applied to the samples to accomplish $7.6*10^{17}$, $1.0*10^{19}$, and $3.9*10^{19}$ n/cm^2. The most important damage mechanism in our samples is driven by the neutron capture reactions by the residual amount of ^{10}B present (less than 0.5%). Lattice defects are created by the recoil of ^{4}He and ^{7}Li, produced by the nuclear reaction, which are emitted isotropically. This makes the defect distribution very homogeneous. After the irradiation, the resistivity progressively increases (16, 64, 124 $\mu\Omega$ cm) and T_c decreases (35.9 K, 24.3 K, and 12.2 K) on increasing the fluence. For sake of comparison low Al-doped samples (5%, 10%, 20%, 30% with a T_c of 36.6 K, 33.4 K, 29.1 K and 24.1 K) were also prepared following a similar procedure [35].

Raman spectra were measured in back-scattering geometry, using a confocal micro-Raman spectrometer equipped with a charge coupled device detector and notch filter to reject the elastically scattered light. The sample was excited by the 632.8 nm line of a 30 mW He-Ne Laser. Raman spectra were collected using a 20x objective (laser spot about 10 μm^2 wide at the sample surface) over the frequency range 200-1100 cm^{-1}, which includes the whole phonon spectral region. For each sample Raman spectra were collected from different points on the sample surface and then averaged to avoid possible effects of preferred microcrystalline orientation.

The Raman spectra of the irradiated and Al-doped samples are shown in Fig.1. Accordingly to literature data [17, 25], the effect of Al doping on the Raman signal is that of driving the onset of a HF spectral structure. The Raman spectra of the irradiated samples, also shown in Fig.1, present an unexpected strong dependence on the fluence, here observed for the first time. Quite interestingly, the two series are surprisingly similar: in both cases, HF structures appear and become dominant at highest values of Al doping or neutron fluence. The same features, occurring at about the same frequencies,
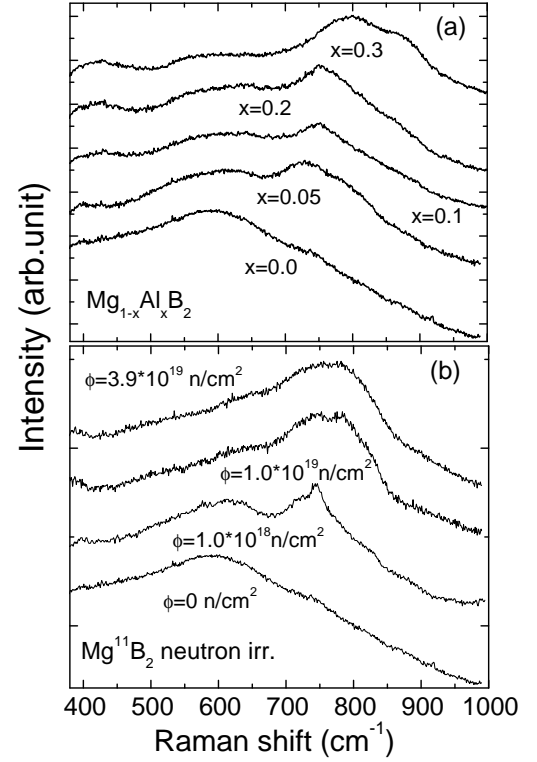

FIG. 1: Background subtracted Raman spectra of Al-doped (a) and neutron irradiated (b) MgB_2 samples. Spectra are shifted upwards of a constant value.

have been observed also in light C-doped MgB_2 [19, 32] and disordered films [33]. Since neutron irradiation has the *only* effect of disordering the lattice, these results suggest that the HF structures in the chemically substituted samples are produced mainly by the lattice disorder as well. In this context, the weak hardening of the frequencies of the HF structures, well detectable only for 30% Al-doped samples, could be likely ascribed to the Al-driven lattice compression.

In light of these results, and because of the unclear origin of the HF structure, the core questions arise: what is the origin of the HF structure and what is the role of the topological disorder to make them visible? And, most importantly, is the **q** = 0 E_{2g} phonon mode the one really probed in the Al-doped and irradiated samples? As we are going to discuss, we believe that the answer to the last question is *negative* and that we are actually probing some kind of phonon density of states.

In Fig. 2 the Raman spectrum of the highest irradiated sample is compared with the PDOS of MgB_2 measured by inelastic neutron scattering [17]. Since no selection rules apply to neutron scattering, the excellent agreement between the experimental data over a wide frequency range (500-1000 cm^{-1}) suggests that in disordered MgB_2, the Raman selection rules are notably relaxed and the Raman spectrum basically reflects the PDOS. On the other
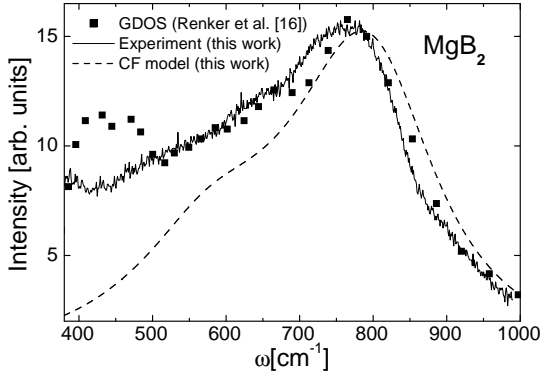
FIG. 2: Raman spectrum of the most irradiated sample (full line) compared with the PDOS from the neutron experiment of Ref. [17](squares) and with the calculated E_{2g} projected PDOS (dashed line). All the reported quantities are empirically normalized to the same peak intensity.
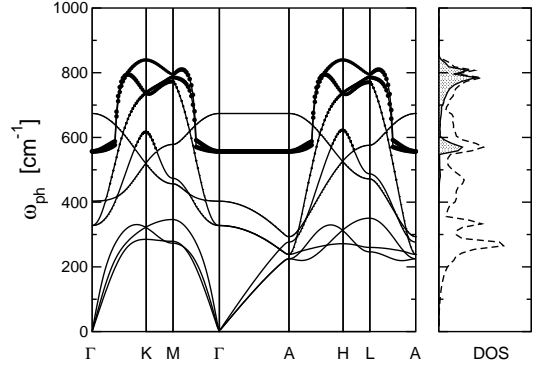

FIG. 3: Left panel: phonon dispersion of MgB_2 within the FC model. The thickness of the lines in the phonon dispersion reflects the magnitude of the E_{2g} component for each mode. Right panel: the corresponding total PDOS (dashed line), and the E_{2g} projected PDOS (shaded area).

side, the apparent disagreement below 500 cm^{-1} suggests a remarkably different weight of the phonon modes in the Raman and the neutron experiment. In the present case we can assume that the topological disorder, induced by neutron irradiation or by chemical substitution, mostly tunes the violation of the Raman momentum selection rules but not of the eigenvector selection.

For a more quantitative check of this empirical hypothesis, we calculated the phonon dispersion of MgB_2 within a force-constant (FC) shell model. Four elastic springs, specified by their tensor connecting B-Mg, Mg-Mg first neighbors, and up to B-B second neighbors were considered. The corresponding twelve parameters were obtained by fitting the first-principle calculated phonon dispersion from Ref. [26]. Since the FC model is meant to reproduce the bare phonon dispersion, in the fitting procedure we did not include the E_{2g} phonon branch along the $\Gamma - A$ direction, which is known to be strongly affected by the el-ph interaction. The effects of the el-ph interaction involving the E_{2g} boron mode with the electronic σ band were included through the self-energy renormalization of the phonon frequencies, by means of the two-dimensional Lindhardt function, which, for the parabolic almost two-dimensional σ bands, results to be a very good approximation. Specific details, as well as the fitting values of the twelve FC parameters, can be found in Ref. [36].

In Fig. 3 we show the so-calculated phonon dispersion curves $\omega_{\mathbf{q},\mu}$ for the different phonon branches μ and the total PDOS (dashed line). Our calculations enable to evaluate the E_{2g} component of each phonon mode, $\eta_{\mathbf{q},\mu}^{E_{2g}} = |\hat{\varepsilon}_{\mathbf{q},\mu} \cdot \hat{\varepsilon}_{E_{2g}}|^2$, which we believe to be effectively probed in our Raman measurements, by simply projecting the generic phonon eigenvector $\hat{\varepsilon}_{\mathbf{q},\mu}$ on the E_{2g} one, $\hat{\varepsilon}_{E_{2g}}$. Thus, in Fig. 3 we show also the E_{2g} character of each phonon branch, as quantified by the thick-

ness of the lines, as well as the E_{2g}-projected phonon densiy of states (E_{2g}-PDOS), shown as shaded area in the right panel. The resulting E_{2g}-PDOS, smeared by a Lorentzian function with width $\Gamma = 100$ cm^{-1}, to simulate the finite phonon lifetime, is also shown in Fig. 2 for comparison purposes. The good agreement between the E_{2g}-PDOS and the Raman spectrum of the highest irradiated sample supports the idea that the topological disorder induces a violation of the Raman momentum selection rules, so that the effective spectra correspond to $\mathbf{q}$-integrated quantities. The slight difference on the low frequency side could be ascribed to secondary contributions, disorder-activated, from other Raman non-active modes, such as the B_{1g}. It is also worth to notice that the peak in the PDOS at about 580-600 cm^{-1} and the HF structures at $\sim$ 800 cm^{-1}, shown in Fig. 3, arise from the contribution of different regions of the Brillouin zone, respectively from the $\mathbf{q}$-states close to the Γ-A and to K-M.

This observation suggests that the onset of the HF structures in the disordered samples could reflect the tuning of the breakdown of the momentum selection rules as induced by the amount of disorder. In this perspective we model the Raman intensity by

$$I(\omega) = \frac{1}{N_c} \sum_{|\mathbf{q}| \le q_c, \mu} \eta_{\mathbf{q},\mu}^{E_{2g}} \frac{1}{\pi} \frac{\Gamma_{q_c}}{(\omega - \omega_{\mathbf{q},\mu})^2 + \Gamma_{q_c}^2}, \quad (1)$$

where N_c is the number of sampling points in the Brillouin zone and where the momentum cut-off q_c depends on the amount of disorder and describes the $\mathbf{q}$-space effectively probed by the Raman measurements. In particular, $q_c \to 0$ for ordered and pure compounds, thus selecting only the Raman $\mathbf{q} = 0$ signal, whereas for highly disordered samples q_c is larger than the size of the Brillouin zone and the total $\mathbf{q}$-integrated PDOS is probed. On a physical ground, we expect that also the phonon scattering rate, Γ_{q_c}, is highly sensitive to the amount of
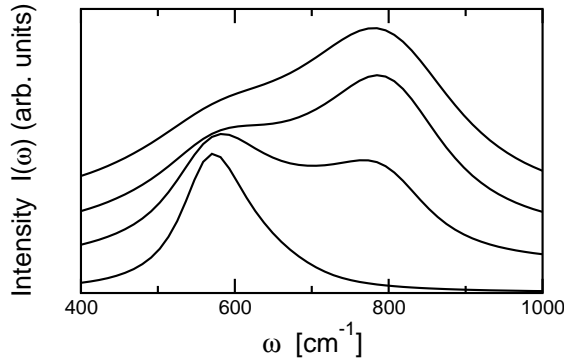
FIG. 4: Raman intensity from Eqs. (1) for different values of the cut-off q_c: (from the bottom to the top) $q_c = 0.30, 0, 45, 0.60, 0.75$ Å^{-1}. Curves are shifted upwards for clarity.

disorder, here parametrized by q_c, with Γ_{q_c} smallest for $q_c \to 0$ and increasing with increasing q_c. To take into account these effects we assumed a linear dependence on q_c, namely $\Gamma_{q_c} = \alpha q_c$, where $\alpha = 120$ Å/cm^{-1}.

In Fig. 4 we show the intensities calculated using Eq. 1 for different values of q_c (0.30, 0,45, 0.60, 0.75 Å^{-1}). For $|\mathbf{q}| \lesssim 0.3$ Å^{-1} we are essentially probing only the flat dispersion region close to the Γ point shown in Fig. 3, and only the low energy structure at ~ 600 cm^{-1} is visible. However, for larger q_c the loss of the momentum selection rules is strong enough to cause probing also of the $|\mathbf{q}|$ states close to the M and K points (we remind that $|\mathbf{q}_{\rm M}| = 0.39$ Å^{-1} and $|\mathbf{q}_{\rm K}| = 0.68$ Å^{-1}), making the HF structure of the E_{2g}-PDOS of Fig. 3 rapidly visible. Finally, for q_c larger than the size of the Brillouin zone, all the $|\mathbf{q}|$ states are equally probed, and the signal $I(\omega)$ approaches the full E_{2g}-PDOS (Fig. 2). The direct experimental *vs.* theoretical comparison in Fig. 2, together with the remarkably similar trend shown by the spectra in Fig. 1 and the calculated intensities in Fig. 4, reveal that, also in disordered systems, the Raman spectrum mostly originates from the E_{2g} phonon branch. Giving the key role of the E_{2g} mode, this finding explains the frequently observed correlation between the Raman signal and the superconducting properties of MgB$_2$ based compounds [17, 19, 25, 32, 33].

In conclusion, in this Letter we presented Raman spectra from differently neutron irradiated and Al-doped MgB$_2$ samples. We have shown that, on increasing the neutron irradiation dose (i.e. topological disorder) as well as Al-doping (i.e. topological disorder plus charge-doping), HF structures appear and rapidly become the dominant spectral features. The remarkable similarity among our spectra and those reported in literature from lightly C-doped samples suggests that the topological disorder, which is unavoidably present in chemically substituted as well as in irradiated sample, is mostly responsible for the modifications of the Raman signal. This is

confirmed by the direct comparison between the Raman spectrum of the most irradiated sample and the neutron PDOS [17]. We also showed that the loss of the Raman momentum selection rules, tuned by the amount of topological disorder, can explain in a natural way the onset of the HF structures. Thus the present results provide a clear and unambiguous explanation of the Raman spectra in MgB$_2$, and address Raman spectroscopy as a very sensitive technique to investigate the role of topological disorder in MgB$_2$ and, more in general, in systems where a strong coupling between the lattice and the electronic degrees of freedom exists. These findings also shed a new light on the interpretation of the previously reported Raman spectra in MgB$_2$ based compounds.

[1] S. L. Budko *et al.*, Phys. Rev. Lett. **86** 1877 (2001)
[2] R. S. Gonnelli *et al.*, Phys. Rev. Lett. **89**, 247004 (2002).
[3] S. Souma *et al.*, Nature (London) **423**, 65 (2003).
[4] A.Y. Liu *et al.*, Phys. Rev. Lett. **87**, 087005 (2001).
[5] H.J. Choi *et al.*, Nature **418**, 758 (2002).
[6] J. Kortus *et al.*, Phys. Rev. Lett. **86**, 4656 (2001).
[7] M. Monni *et al.*, cond-mat/0506162.
[8] J. M. An and W. E. Pickett Phys. Rev. Lett. **86**, 4366 (2001).
[9] Y. Kong *et al.*, Phys. Rev. B **64**, 020501(R) (2001).
[10] T Yildirim *et al.*, Phys. Rev. Lett. **87** 037001 (2001).
[11] A. F. Goncharov *et al.*, Phys. Rev. B **64**, 100509(R) (2001).
[12] D. Di Castro *et al.*, Phys. Rev. B **72**, 094504 (2005).
[13] Y. Bugoslavsky *et al.*, Nature **411**, 561 (2001)
[14] M. Eisterer *et al.*, Supercond. Sci. Technol. **15**, L9-L12 (2002).
[15] M. Putti *et al.*, Appl. Phys. Lett. **86**, 112503 (2005).
[16] D. Di Castro *et al.*, Europhys. Lett. **58**(2), 278 (2002).
[17] B. Renker *et al.*, Phys. Rev. Lett. **88**, 067001 (2002).
[18] T. Masui *et al.*, Phys. Rev. B **70**, 024504 (2004).
[19] J. Arvanitidis *et al.*, J. Phys. Chem. Solids **65**, 73 (2004).
[20] O. de la Pena *et al.*, Phys. Rev. B **66**, 012511 (2002).
[21] G. Profeta *et al.*, Phys. Rev. B **68**, 144508 (2003).
[22] J. Kortus *et al.*, Phys. Rev. Lett. **94**, 027002 (2005).
[23] S.C. Erwin, and I.I. Mazin, Phys. Rev. B **68**, 132505 (2003).
[24] K. Kunc *et al.*, J. Phys. Condens. Matter **13**, 9945 (2001).
[25] P. Postorino *et al.*, Phys. Rev. B **65**, 020507(R) (2001).
[26] K. P. Bohnen *et al.*, Phys. Rev. Lett. **86**, 5771 (2001).
[27] G. Satta *et al.*, Phys. Rev. B **64**, 104507 (2001).
[28] X. Chen *et al.*, Phys. Rev. Lett. **87**, 157002 (2001).
[29] M. Calandra and F. Mauri Phys. Rev. B **71**, 064501 (2005).
[30] H. Martinho *et al.*, Solid State Comm. **125**, 499 (2003) .
[31] E. Cappelluti, cond-mat/0512198 (2005).
[32] D. A. Tenne *et al.*, Phys. Rev. B **71**, 132512 (2005).
[33] K. A. Yates *et al.*, Phys. Rev. B **68**, 220512(R) (2003).
[34] A.V. Pogrebnyakov *et al.*, Phys. Rev. Lett. **93**, 147006 (2004).
[35] M. Putti *et al.*, Phys. Rev. B **71**, 144505 (2005).
[36] G. Campi *et al.*, cond-mat/0601656 (2006).